Liquid Crystals
Publication details, including instructions for authors and subscription information:
http://www.informaworld.com/smpp/title~content=t713926090

New mesogens with cubic phases: hydrogen-bonded bipyridines and siloxane-containing benzoic acids II. Structural studies

Etsushi Nishikawa[a]; Edward T. Samulski[a]
[a] Venable and Kenan Laboratories, Department of Chemistry CB#3290, The University of North Carolina at Chapel Hill, Chapel Hill, NC 27599-3290, USA,

Online publication date: 06 August 2010

To cite this Article Nishikawa, Etsushi and Samulski, Edward T.(2000) 'New mesogens with cubic phases: hydrogen-bonded bipyridines and siloxane-containing benzoic acids II. Structural studies', Liquid Crystals, 27: 11, 1463 — 1471
To link to this Article: DOI: 10.1080/026782900750018627
URL: http://dx.doi.org/10.1080/026782900750018627

LIQUID CRYSTALS, 2000, VOL. 27, NO. 11, 1463–1471

New mesogens with cubic phases: hydrogen-bonded bipyridines and siloxane-containing benzoic acids II. Structural studies

ETSUSHI NISHIKAWA and EDWARD T. SAMULSKI*

Venable and Kenan Laboratories, Department of Chemistry CB#3290, The University of North Carolina at Chapel Hill, Chapel Hill, NC 27599-3290, USA

(*Received 1 April 2000; accepted 12 May 2000*)

The supramolecular structure of new hydrogen-bonded mesogens composed of dipyridyl and 4-(oligodimethylsiloxyl)alkoxybenzoic acids was investigated by X-ray diffraction and deuterium NMR. These H-bonded mesogens exhibit a cubic thermotropic liquid crystalline phase at a temperature below a smectic A phase. Moreover, above the smectic A phase two optically isotropic, low viscosity phases (I_1 and I_2) exist with the lower temperature I_1 phase comprising aggregated mesogens. Two broad, temperature-independent, wide angle X-ray reflections suggest that the aggregation is driven by nanophase-separation; the aggregate adopts a structure with one domain siloxane rich and the other hydrocarbon rich. In the isotropic melt near the I_1-to-I_2 phase transition, a very weak small angle reflection, indicates incipient lamellar-like clustering of the aggregated mesogens. With decreasing temperature the intensity of the small angle reflection increases and in the smectic A phase, the reflection becomes very sharp. In the cubic phase the small angle reflection splits into two peaks which can be indexed with a face-centred cubic (FCC) structure. The deuterium NMR measurements in the isotropic and smectic A phases are indicative of aggregation and an oriented, lamellar-like structure, respectively. In the cubic phase, the collapse of quadrupolar splittings is consistent with an isotropic average of the quadrupole interaction caused by mesogen translational diffusion through a cubic supramolecular structure.

1. Introduction

In the first part of this work we described the formation of cubic phases in new hydrogen-bonded mesogens based on 4-(oligodimethylsiloxyl)alkoxybenzoic acids and 4,4′-dipyridyl ('bipyridine'). The stoichimetric 2:1 complexes show thermotropic cubic phases over a moderate temperature range (below 100°C) [1]. Abbreviated Si_nC_mBA, where n indicates the number of siloxyl units and m the number of methylenes linking the former to the *para*-position of the benzoic acid, these siloxyl-terminated acids have flexible, bulky, and nonpolar termini (siloxyl tails). The siloxyl tails are highly incompatible with the H-bonded, aromatic benzoic acid/bipyridine mesogenic cores, and in the melt chemical incompatibility can lead to aggregation wherein the chemically distinct components are nanophase-separated. Moreover, aggregate formation might underlie the formation of a cubic supramolecular structure found in these and related mesogenic materials. Here we investigate the cubic phase exhibited by a new 4-(oligodimethylsiloxyl)alkoxybenzoic acid having a branched siloxane terminal tail, tSi_3C_6BA, in a 2:1 complex with dipyridyl, tSi_3C_6BA-BiPy (figure 1). Deuterium nuclear magnetic resonance (D-NMR) and X-ray diffraction give new insights into the structure of the building blocks (aggregates) and symmetry of the space group in the cubic mesophase.

The well known cubic phases of 4′-*n*-alkoxy-3′-nitrobiphenyl-4-carboxylic acids (ANBC-*n*, where n is the number of carbon atoms in the alkoxy chain) were first reported more than four decades ago [2, 3]. In these materials the nitrobiphenylbenzoic acid moiety dimerizes into a cyclic, H-bonded, rectilinear structure that comprises a polar mesogenic core terminating with long, aliphatic tails. These two chemically distinct moieties—the polar aromatic core and the apolar aliphatic tails—comprising ANBC-*n* should tend to segregate from each other to form nanophase-separated supramolecular structures. Other known liquid crystals exhibiting cubic phases also have chemically differentiated architectures with structural similarities to the ANBC-*n* series and to our new siloxane-based Si_nC_mBA mesogens [4–7]. Therefore it is reasonable to assume that one of the

*Author for correspondence; e-mail: et@unc.edu

Liquid Crystals ISSN 0267-8292 print/ISSN 1366-5855 online © 2000 Taylor & Francis Ltd
http://www.tandf.co.uk/journals

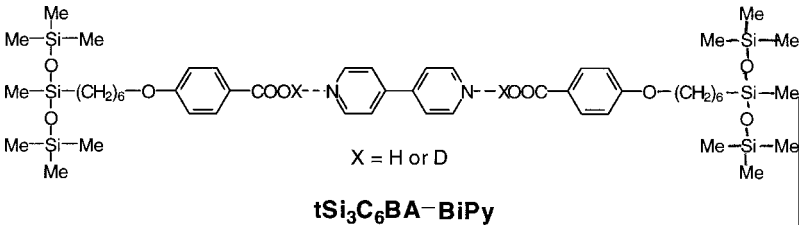

Figure 1. Structural formula of the hydrogen-bonded mesogen under investigation (tSi_3C_6BA-BiPy).

important prerequisites for thermotropic cubic phase formation is indeed nanophase separation driven by incompatible chemical constitutions of the mesogen.

The structure of the cubic phase of the ANBC-*n* series and other compounds has been intensively investigated by X-ray diffraction and NMR [8–10]. Tardieu and Billard identified *Ia*3*d* to be the space group of the cubic phase observed in the hexadecyloxy derivative, ANBC-16 [11]. Some phasmidic molecules with four aliphatic chains, each with eight to twelve carbons, have cubic phases with *Im*3*m* symmetry [12]. Silver (I) complexes of alkoxystilbazoles with alkylsulphate counter anions exhibit *Ia*3*d* cubic phases [13, 14]. The architecture of the supramolecular structure in the cubic phases exhibited by the ANBC-*n* series seems to consist of interpenetrating jointed-rods [11], rather than close-packed spherical micelles [8] or an unconnected infinite-rod model [15]. The jointed-rod model of the cubic phase of ANBC-*n* is also consonant with nitrogen NMR investigations [16].

In this paper we investigate the structure of the cubic phase of the hydrogen-bonded Si_nC_mBA mesogens using D NMR and X-ray diffraction (XRD). As anticipated, the hydrogen-bonded complex of dipyridyl with the siloxane-containing benzoic acid exhibits a nanophase-separated supramolecular structure that is confirmed with wide angle XRD. Additionally the X-ray reflection pattern at small angles supports a face-centred cubic (FCC) structure in the cubic mesophase. By contrasting D NMR measurements in conventional nematic mesophases of siloxane-based, H-bonded acids with observations in the smectic and cubic phases of the Si_nC_mBA mesogens, we can begin to infer some structural attributes of the aggregates that dominate the behaviour of these unusual liquid crystals.

2. Experimental

2.1. *Measurements*

Differential scanning calorimetry data were recorded with a Seiko Denshi DSC-220 at a heating/cooling rate of 5 K min^{-1}. The observation of textures was performed using a Nikon Microphot-FX microscope equipped with a Mettler FP-82HT (or a Linkam TMS-90) hot stage and a Sony CCD-IRIS video camera. XRD measurements were performed with monochromatic CuK_α radiation (wavelength 1.54 Å) from the X-ray generator with a power of 100 W (25 mA × 40 kV). A two-dimensional imaging plate system was used as detector (2500 × 2500 pixels, 80 μm resolution).

Deuterium NMR measurements were carried out with a Bruker 500 MHz spectrometer. The tSi_3C_6BA acid proton was exchanged by heating in ethanol-d_1 and crystallizing from D_2O.

2.2. *Materials*

The chemical structure of the hydrogen-bonded tSi_3C_6BA-DiPy complex under investigation is shown in figure 1. The mesogen's termini in this complex are branched siloxane moieties; in our first paper we reported hydrogen-bonded Si_nC_mBA mesogens having tails comprising linear siloxane moieties [1]. In order to investigate the structure of cubic mesophases exhibited by this class of H-bonded Si_nC_mBA mesogens, we selected the acid with the branched siloxane tail (tSi_3C_6BA) as the tSi_3C_6BA-BiPy complex had a cubic phase over a broad temperature range (about 30°). The siloxane-containing benzoic acid and the dipyridyl complex were prepared using the same synthetic procedures as reported for the linear Si_nC_mBA analogues [1].

The phase behaviour of the hydrogen-bonded complex was determined with DSC and optical microscopy. Figure 2 shows the DSC traces on heating and on cooling along with the phase sequence and phase transformation temperatures. On cooling from the isotropic phase, a smectic A phase appears at 90°C. In figure 3(*a*) the focal-conic texture of the smectic A phase is shown. On further cooling the phase transformation from smectic A to cubic phase takes place at about 86°C. This transformation cannot be detected with DSC. However, the transition is clearly observed with optical microscopy—the optically extinct areas of the cubic phase start developing in the birefringent smectic A phase as shown in figure 3(*b*). Subsequently a phase transformation to a highly ordered smectic takes place at 53°C. The temperature range of the cubic phase of tSi_3C_6BA-BiPy extends for some 33°, which is much broader than cubic phases observed for the linear Si_nC_mBA siloxane acid complexes [1]. Finally crystallization occurs at 43°C. On heating, the same phase sequence is observed as shown in figure 2.

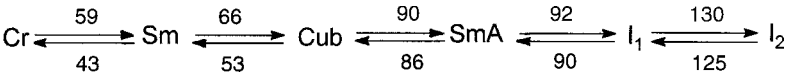

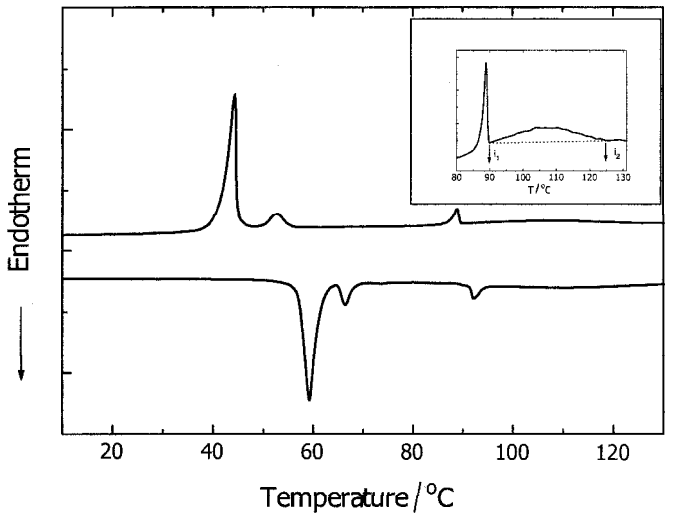

Figure 2. DSC traces (heating/cooling rates of 5 K min^{-1}) of the tSi_3C_6BA-BiPy complex.

3. Results

3.1. *X-ray diffraction*

In order to investigate details of the supramolecular structure of the tSi_3C_6BA-BiPy mesogen, temperature-dependent XRD measurements were carried out. While it is difficult to resolve on typical vertical scale expansions, the DSC measurements indicate a broad transition in the nominally 'isotropic' melt of tSi_3C_6BA-BiPy (see inset in figure 2). That is, above the smectic A to isotropic phase transition (I_1), the stoichiometric tSi_3C_6BA-BiPy complex appears to be aggregated, and on heating this isotropic phase the aggregate breaks down into a fluid of discrete, H-bonded complexes. This dis-aggregation transformation appears to be complete only above $I_2 \approx 130$°C. Thus there are two optically isotropic states above the smectic A phase, I_1 consisting of some type of aggregated H-bonded complexes, and a higher temperature phase I_2 without aggregation. (Presumably the H-bonded complex is still intact above I_2, although the higher the temperature, the more the equilibrium shifts from the H-bonded complex to the unassociated components.)

The long range order in these two isotropic phases, as well as that in the cubic phase appearing below the smectic A phase, could be studied with CRD. In figure 4 the intensity profiles observed at temperatures of 125, 95, 90 and 80°C are reported. We observe broad, wide angle reflections ($2\theta > 10°$) with two maxima at $2\theta \approx 12.5°$ and $2\theta \approx 17.5°$, which correspond to intermolecular spacings of ≈ 7 and ≈ 5 Å, respectively. Moreover, both the intensity and the peak position of the reflections at wide angles are unaffected by a change of temperature. This behaviour is anticipated for reflections associated with nearest-neighbour intermolecular separations, and correspondingly the reflection with the spacing of ≈ 7 Å is assigned to the scattering from intermolecular spacings within the tSi_3C_6BA siloxane-rich nanophase, while the ≈ 5 Å reflection is attributed to intermolecular distances within the mesogenic core-rich nanophase [17, 18]. This two-component wide angle result supports an arrangement of complex mesogens wherein the H-bonded aromatic cores seggregate from the bulky siloxane moiety. Additionally, this nanophase-separated supramolecular aggregate persists at temperatures above I_1 and is observed over the whole I_1 temperature range, even at 125°C near the I_1 to I_2 transition temperature, see figure 4 (*a*).

We also observe a reflection at small angles ($2\theta \approx 2.4°$) at 125°C. However, the intensity is very weak and the width of the reflection is very broad. This could be the signature of an incipient stratification of aggregate clusters in the I_1 phase. On cooling deeper into the I_1 phase, the small angle intensity increases as seen in the 95°C diffraction scan, figure 4 (*b*). In the smectic A phase at 90°C, the small angle reflection shows a strong, well resolved reflection with a maximum of $2\theta \approx 2.2°$; this corresponds to strata with a spacing of 40 Å, figure 4 (*c*). However, on cooling to 80°C into the cubic phase, the small angle reflection splits into two peaks with maxima located at $2\theta \approx 2.3°$ and 2.0°, figure 4 (*d*). Moreover, at

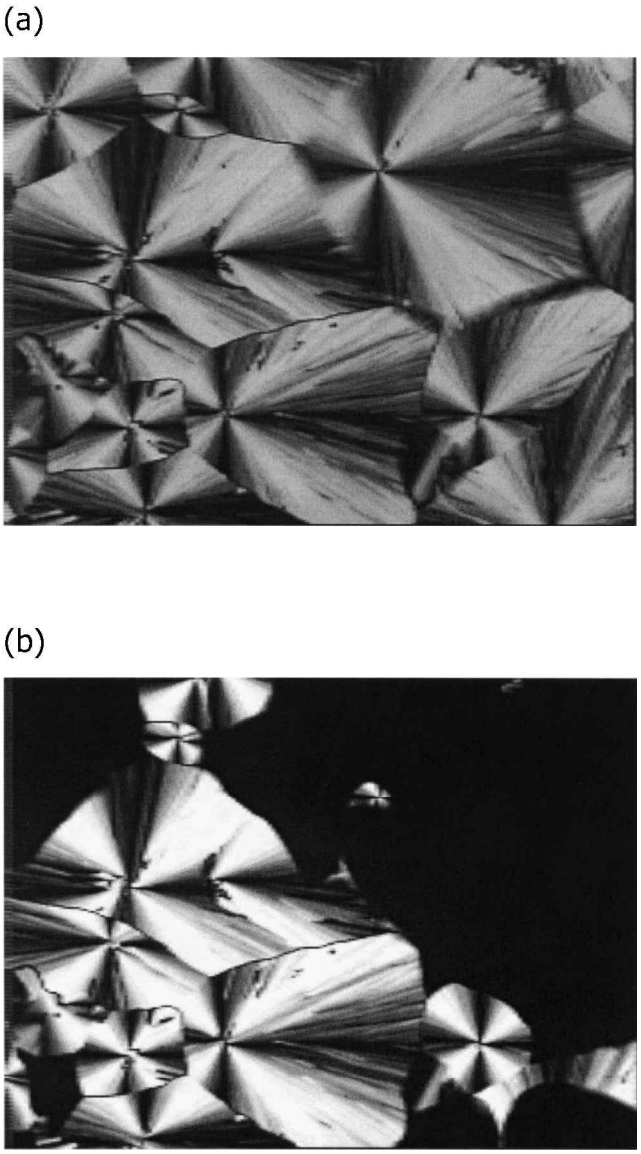

Figure 3. Texture of the tSi_3C_6BA-BiPy complex observed by polarized optical microscopy: (*a*) the smectic A phase, (*b*) the cubic phase growing into a field of the smectic A phase.

this temperature we observe a change of the azimuthal intensity distribution of the X-ray pattern for the small angle reflections. In the smectic A phase the azimuthal intensity is uniform and exhibits a continuous circular pattern indicative of isotropically oriented lamellae. This uniform azimuthal intensity coalesces into discrete spot reflections in the cubic phase. This fragmentation of the small angle azimuthal intensity into discrete reflections is evidence for a well defined supramolecular organization in the cubic liquid crystalline phase of the 2:1 tSi_3C_6BA-BiPy complex.

3.2. *Deuterium NMR*

Deuterium NMR (D NMR) gives information about both the local and the larger scale orientational order in a mesophase. The magnitude of the quadrupolar interaction, a measure of the motionally-averaged electric field gradient at the deuterium nucleus, is determined by local librations of the mesogen and reorientations in the orientationally anisotropic mean field of the mesophase. The average also reflects larger scale motions: mesogen translation (self-diffusion) through the topology of the supramolecular structure of the phase. An example of the latter kind of averaging might be, for example, reorientational averaging caused by translational diffusion of a mesogen in a cholesteric liquid crystal along the helix axis of its helicoidal supramolecular arrangement.

We carried out deuterium NMR measurements of symmetric, H-bonded complexes of tSi_3C_6BA with dipyridyl (and perdeuterated dipyridyl-d_8) wherein the carboxylic acid protons have been exchanged with deuterium (tSi_3C_6BA-d_1), and with the asymmetric, non-cubic phase-forming mesogen based on a 1:1 tSi_3C_6BA-d_1: 4-phenylpyridine complex. It is instructive to first consider the D NMR observations for the tSi_3C_6BA-d_1: 4-phenylpyridine complex, as this mesogen forms a conventional nematic phase. On cooling from the isotropic-to-nematic phase transition, a quadrupolar splitting $\Delta\nu$ (= 127 kHz) is observed. In the case of the deuteron label in the O–D ··· N hydrogen bond, the quadrupolar splitting can be readily translated into a measure of the mesogen order parameter (S). S characterizes the orientational order of the 'long molecular axis' (**m**) of the mesogen since the principal value of the electric field gradient (efg) tensor is along the O–D ··· N hydrogen bond, which in turn is essentially coincident with **m** in the complex. The expression relating $\Delta\nu$ to S given by

$$\Delta\nu = 2\nu_q S P_2(\cos\Omega) \qquad (1)$$

where the quadrupolar interaction constant is $\nu_q = 3e^2qQ/4h$ (~93 kHz for a O–D bond in an aromatic acid [19]) and we assume an axially symmetric local efg tensor. The order parameter $S = \langle P_2(\cos\theta)\rangle = \langle (3\cos^2\theta - 1)/2\rangle$ signifies an average of the O–D ··· N bond direction (i.e. the mesogen **m**-axis) over its anisotropic motion. The angle θ is the instantaneous angle between the **m**-axis and **n**, the local director in the mesophase; Ω is the angle between the magnetic field **B** and **n**. For the positive diamagnetic anisotropy anticipated for the nematic phase of the 1:1 tSi_3C_6BA-d_1:4-phenylpyridine complex, the nematic director **n** should be aligned along the NMR spectrometer magnetic field ($\Omega = 0°$) resulting in $P_2(\cos\Omega) = 1$ in equation (1). Figure 5 shows the typical increase for $\Delta\nu$ on cooling the tSi_3C_6BA-d_1:4-phenylpyridine nematic. The order parameter at the I–N phase

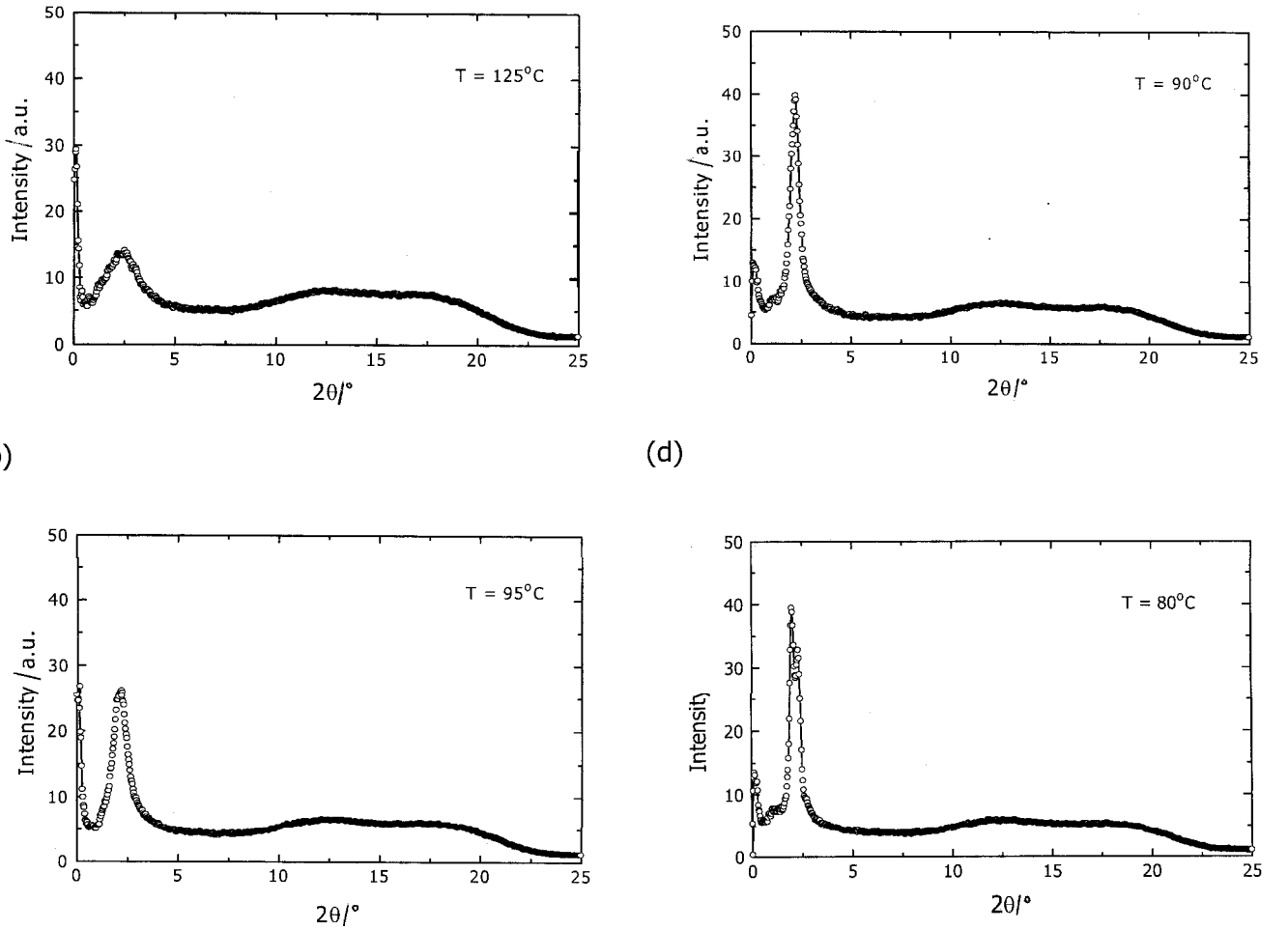

Figure 4. X-ray intensity profiles of the tSi_3C_6BA-BiPy complex observed at a temperature of (*a*) 125, (*b*) 95, (*c*) 90 and (*d*) 80°C.

transition is $S = \Delta\nu_{obs}/2\nu_q = 127\,kHz/186\,kHz = 0.7$; this is a little high and may reflect uncertainties in the value of ν_q for the actual H-bonded deuteron in the complex, i.e. uncertainties in the magnitude of the static efg tensor for the O–D ··· N bond.

In figure 6 we show the D NMR spectra of the 2:1 tSi_3C_6BA-d_1 : dipyridyl complex on cooling from the isotropic phase into the smectic A phase and ultimately into the cubic phase. In the I_1 phase at 102°C a singlet is observed and this persists down to 92°C, about 3 degrees above the I_1-to-smectic A transition. The linewidth of the resonance (~ 1100 Hz at 102°C) doubles on decreasing the temperature to 92°C. Apparently the reorientation of the mesogen in the I_1 phase slows significantly due to aggregation, resulting in a loss of efficacy for the isotropic average of the quadrupolar interaction. At 89°C the smectic A phase appears and the associated quadrupolar splitting of this oriented, uniaxial phase is apparent. Note however, that the quadrupolar splitting $\Delta\nu = 26\,kHz$ in this smectic A phase is more than a factor of five times *smaller* than that observed in the nematic phase of the asymmetrical tSi_3C_6BA-d_1 : phenylpyridine mesogen. Typically smectics are *more* ordered than nematics so obviously there is another mode of averaging operative in this smectic A phase. In the cubic phase the quadrupolar doublet collapses as shown in the spectra at 82°C (figure 6). The linewidth of the resonance in the cubic phase (~ 5500 Hz at 82°C) is much broader than that in the isotropic I_1 phase and increases on cooling deeper into the cubic phase. This collapse of the quadrupolar splitting is consonant with nearly isotropic averaging of the quadrupolar interaction by translational diffusion of the mesogen on a mesoscopic scale, one having a supramolecular structure

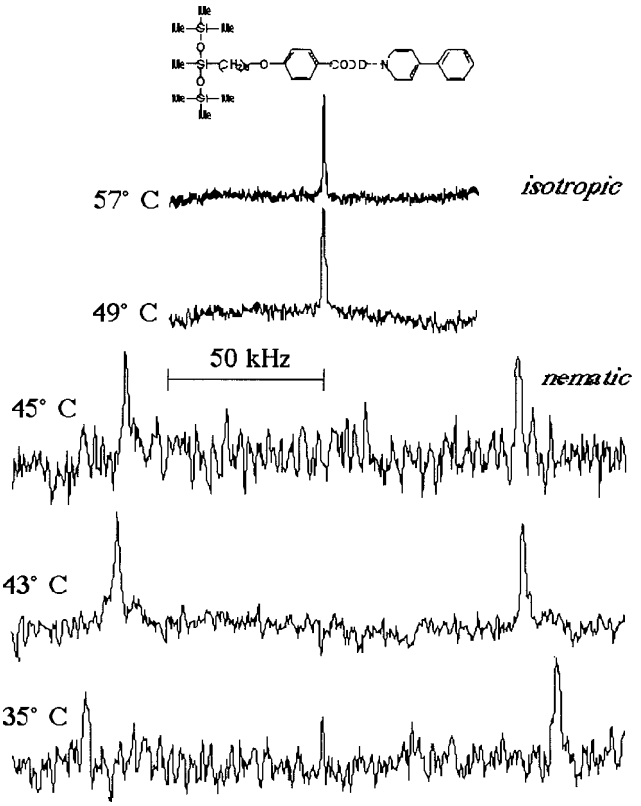

Figure 5. Deuterium NMR spectra of the acid-exchanged asymmetric, H-bonded 1:1 tSi_3C_6BA-d_1:4-phenylpyridine mesogen in its isotropic and nematic phases.

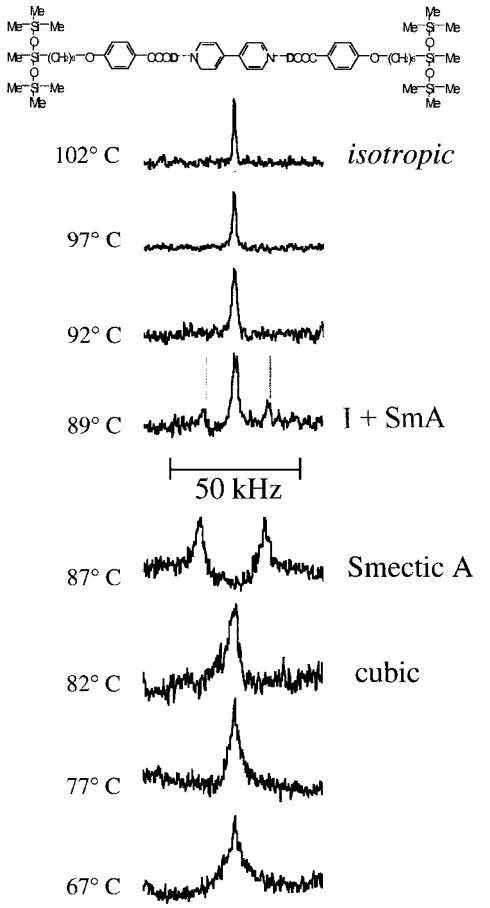

Figure 6. Deuterium NMR spectra of acid-exchanged tSi_3C_6BA-d_1 BiPy as a function of temperature. There is increased broadening of the resonance on cooling in the isotropic phase. A quadrupolar splitting appears in the smectic A phase, which in turn collapses to a singlet on cooling into the cubic phase.

with cubic symmetry. This observation is reminiscent of reported deuterium NMR studies of molecular averaging in the cubic 'blue phase' found in esters of cholesterol [20].

Similar results are observed when the deuterium label is covalently associated with the complex mesogenic core. In figure 7 we show the D NMR spectra of the tSi_3C_6BA:dipyridyl-d_8 complex as a function of temperature. The appearance of the chemically-shifted resonances in the isotropic phase derives from the inequivalence of deuterons *ortho* and *meta* to the nitrogen in dipyridyl. On cooling in the isotropic phase there is evidence of line broadening suggestive of less efficacious averaging and consistent with aggregation of the complex mesogens. As a result of geometrical inequivalence of the two types of deuterons (with respect to the C–D bond orientation relative to the dipyridine *para* axis), two sets of quadrupolar doublets are observed in the smectic A phase (between 88 and 83°C; we are not able to identify the isotropic impurity that persists in the spectra). The quadrupolar doublets collapse when the mesophase is cooled into the cubic phase (81°C). The resonance persists as a broad line into the uncharacterized smectic phase below the cubic phase (the spectrum at 51°C in figure 7).

4. Discussion

The results of the wide angle XRD measurements indicate that the tSi_3C_6BA-BiPy mesogens exhibit nanophase separation of their chemically incompatible moieties throughout the whole temperature range, even in the isotropic I_1 phase where aggregation appears to be a precursor to smectic A mesophase formation. The relatively strong reflection at small angles in the I_1 phase indicates that although this phase is nominally isotropic and possesses low viscosity, it exhibits indications of the formation of long range, lamellar-like supramolecular organization on lowering the temperature. In the smectic A phase a well defined layer spacing of 40 Å is observed; the molecular contour length of the symmetric tSi_3C_6BA:dipyridyl complex is about 48 Å. This means that the lamellae probably consist of a partially interdigitated arrangement of mesogen tails (i.e., a SmA_d type arrangement).

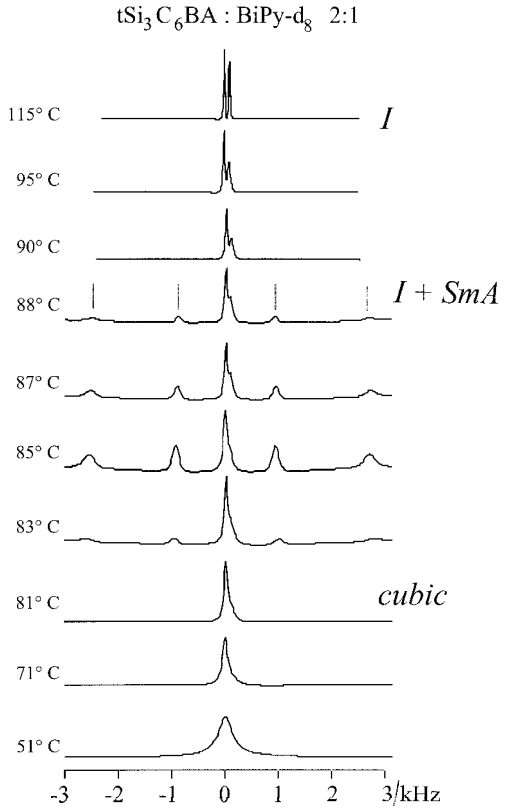

Figure 7. Deuterium NMR spectra of tSi_3C_6BA : dipyridyl-d_8 as a function of temperature. There is increased broadening of the chemically shifted *ortho*- and *meta*-deuterons in dipyridyl on cooling in the isotropic phase. Two quadrupolar splittings appear in the smectic A phase, which in turn collapse on cooling into the cubic phase.

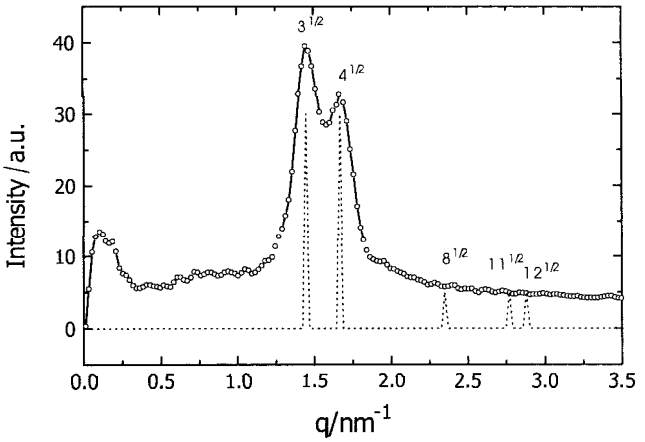

Figure 8. X-ray intensity profile of the tSi_3C_6BA-BiPy complex in the cubic phase at a temperature of 80°C. The dotted lines show the calculated reflection positions of the face-centered cubic structure.

In the cubic phase the small angle reflection corresponding to the smectic layer periodicity breaks into two small angle reflections ($2\theta \approx 2.0°$ and $2\theta \approx 2.3°$), which correspond to spacings of $d = 43.5$ Å and $d = 38$ Å, respectively. The intensity profile in the region of $0 < q < 3.5\,nm^{-1}$ [$q = (4\pi \sin\theta)/\lambda$, λ is the wavelength] is shown in figure 8. The positions of the reflections of several cubic systems were simulated (without considering relative intensities). We find that the small angle reflections in the cubic phase of the symmetric tSi_3C_6BA : dipyridyl mesogen can be rationalized if a face-centered cubic (FCC) close packing structure is posited. The positions of the simulated reflections of the FCC structure are shown as dotted lines in figure 8. While the reflection patterns is very similar to that previously reported in FCC structures of aggregated polyelectrolyte–surfactant complexes [21], the quality of the data does not enable us to differentiate among the 11 space groups having the FCC unit cell. From our analysis we conclude that the reflections at $q = 1.45$ and $1.65\,nm^{-1}$ correspond to the (1 1 1) and (2 0 0) reflections, respectively. Using the relation $1/d_{hkl} = 1/a(h^2 + k^2 + l^2)^{1/2}$, the calculated dimension of the FCC unit cell, $a = 7.5$ nm, is approximately twice the molecular length of the H-bonded mesogen.

The D NMR experiments show that in the smectic A phase of the symmetric tSi_3C_6BA : dipyridyl mesogen there is an extra averaging process relative to the motions operative in the conventional nematic formed by the asymmetric mesogen tSi_3C_6BA-d_1 : 4-phenylpyridine. One can envisage idealized lamellar architectures wherein the motional averaging of the molecular long axis **m** relative to the spectrometer field **B** may be influenced by molecular diffusion. In figure 9 we contrast the relative magnitudes for expected efg tensor components in an aggregate-fixed x,y,z-frame defined relative to the local director **n**. For an infinite lamellar sheet where the principal value of local C–D efg tensor is coincident with molecular long axis **m** and in turn, **m** is approximately parallel to **n**, one observes the maximum quadrupolar interaction when **n**$\parallel$ **B** ($\Omega = 0°$ in equation (1)). For this orientation the principal values of the (relative) efg tensor are $(-1/2, -1/2, +\mathbf{1})$ with the **z**-component along the field, figure 9 (*a*) left. For the case where the lamellae are tangent to **B** ($\Omega = 90°$), the **z**-component is $-\mathbf{1/2}$ and the magnitude of the observed $\Delta\nu$ would be decreased by 1/2 figure 9 (*a*) right. In both cases mesogen translational motion does not further average the quadrupolar interaction. In the case of an infinite cylindrical architecture, figure 9 (*b*), with the cylinder axis along **B**, $\Delta\nu$ also would be decreased by 1/2 since again there is no influence on the motional average from translational diffusion as **n** (and **m**) are always perpendicular to **B** for this orientation of the cylindrical supramolecular structure. However if the cylinder axis is perpendicular to **B**, translation (self-diffusion) leads to the reorientation of **m** relative to **B** and averages the $+1$ and $-1/2$ efg

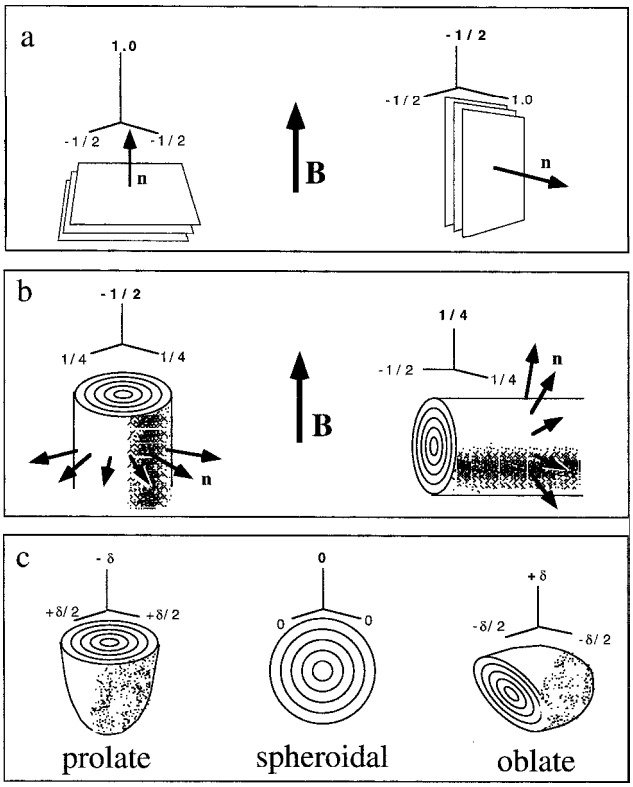

Figure 9. Schematic depiction of the principal axis system of the motionally averaged electric field gradient tensor defined in the aggregate-fixed x,y,z-frame with the (relative) magnitude of its principal value $|\mathbf{z}|$ shown in boldface; $\mathbf{z} \| \mathbf{B}$, the spectrometer magnetic field. The tensors are shown for a statified mesophase wherein the local O–D bond efg tensor has is principal value along the 'molecular long axis' (**m**) and the molecules are normal to the lamellae, i.e. the molecular long axis is parallel to **n**, where **n** is the local director—the normal to the lamellae. Panel (*a*) shows a perpendicularly aligned lamellar supramolecular structure (left) and a tangentially aligned supramolecular structure (right). In (*b*) the cylindrical supramolecular arrangement of concentric lamellae has its cylinder axis along (left) and normal (right) to the magnetic field. In (*c*) distorted prolate and oblate spheroidal 'multi-lamellar vesicles' are shown.

tensor components to give a diffusionally averaged efg $(-1/2, +1/4, +\mathbf{1/4})$. In this orientation we expect translation to decreases $\Delta\nu$ by the factor 1/4 relative to $\Delta\nu$ found in the normally oriented lamellae, figure 9 (*a*). Lastly, in figure 9 (*c*) new modes of diffusional averaging of the efg tensor are introduced when the lamellar aggregates have finite dimensions. Decreasing the aspect ratio of spheroidal shaped aggregates will enable diffusion to more effectively average the efg tensor, averaging it to zero in the case of a sphere.

In order to achieve the rather large reduction in $\Delta\nu$ found in the smectic A phase of the symmetric tSi_3C_6BA : dipyridyl mesogen ($\Delta\nu_{obs} = 26$ kHz) relative to that in the nematic phase of the asymmetric, non-cubic-phase forming mesogen $tSi_3C_6BA\text{-}d_1$: 4-phenylpyridine ($\Delta\nu_{obs} \sim 140$ kHz), we have to postulate an architecture for the smectic A phase that has the possibility of extra degrees of diffusional averaging. One example could be a smectic A consisting of oriented, lamellar-like mesostructures—oblate bi- or multi-lamellae aggregates. A cartoon of such a putative architecture is shown in figure 10. This shows schematically how on cooling from the isotropic phases (I_1 and I_2) the equilibrium shifts initially to H-bonded, dimeric mesogens and eventually nanophase separation followed by oblate bicelle aggregation into a lamellar-like arrangement. On further cooling into the cubic phase, the collapse of the quadrupolar doublet (figures 6 and 7) corresponds to a transformation of the oblate aggregates into an architecture with cubic symmetry. In the cartoon this is represented schematically as cubic packing of spherical 'vesicles.' We recognize however, that there is a large taxonomy of bicontinuous

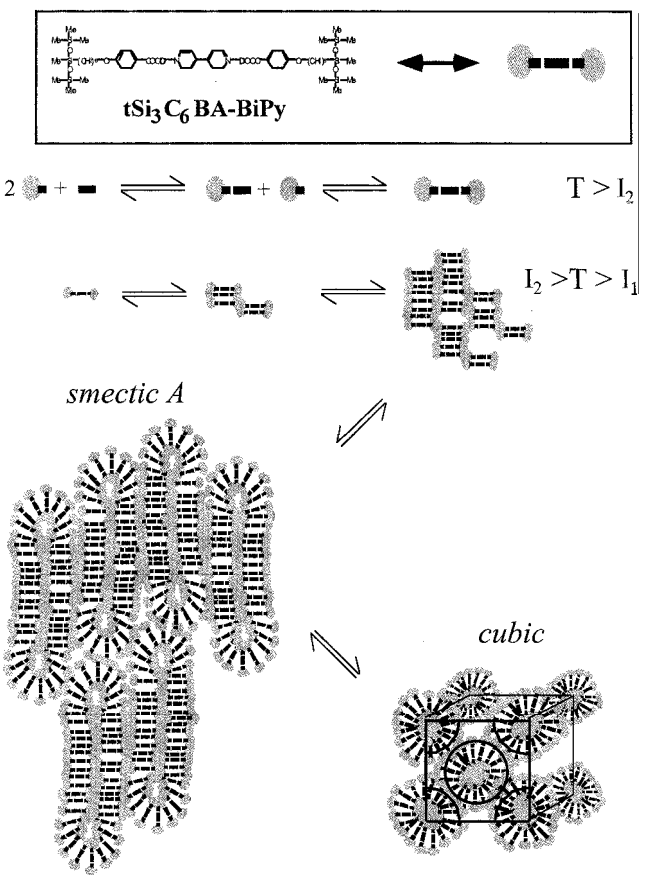

Figure 10. A schematic representation of the H-bonded tSi_3C_6BA-BiPy complex mesogen and its associated equilibria including: association of the acid and bipyridine ($T > I_2$); aggregation of mesogens into nanophase-separated aggregates ($I_2 > T > I_1$); stacking of oblate bicelles to form a lamellar smectic A phase; and the eventual transformation of the smectic A to a cubic architecture.

architectures having cubic symmetry while maintaining the option of nanophase-separated components [22]. In all of such architectures the quadrupolar interaction would be averaged to zero via mesogen translational motion.

5. Concluding remarks

We conclude that a FCC mesostructure accounts for the cubic phase observed in a new class of thermotropic, hydrogen-bonded mesogens derived from 2:1 mixtures of siloxane-substituted benzoic acids with dipyridyl. The nanophase separation that drives the aggregation persists above the mesophase—in an isotropic phase—for some 35° above the smectic A to isotropic phase transition. Line broadening in the NMR spectra when the isotropic liquid is cooled supports the concept of H-bonded mesogens aggregating prior to mesophase formation. XRD supports the build-up of interlamellae scattering on cooling the isotropic liquid into the smectic A phase. Below the smectic A phase both the X-ray and NMR data give unequivocal evidence for the presence of a supramolecular structure having, respectively, static and dynamic cubic symmetry. It may be possible that a more refined picture of the supramolecular structure in the cubic phase of the tSi_3C_6BA:dipyridyl mesogen might be derived from neutron scattering studies that contrast the scattering from the protonated mesogenic core with that derived from the deuterium-labelled tSi_3C_6BA:dipyridyl-d_8 complex.

We are indebted to Prof. O. Zhou for sharing his X-ray facilities. We are grateful to C. D. Poon, D. Williams and C. Murray for helping with the D NMR experiments. This work was supported in part by NSF (DMR-9971143).

References

[1] Nishikawa, E., and Samulski, E. T., 2000, *Liq. Cryst.*, **27,** 1457.
[2] Gray, G. W., Jones, B., and Narson, F., 1957, *J. chem. Soc.*, 393.
[3] Demus, D., Kunicke, G., Keelsen, J., and Sackmann, A., 1968, *Z. Naturforsch.*, **23a,** 84.
[4] Bluce, D. W., Dunmur, D. A., Hudson, S. A., Maitlis, O. M., and Styring, P., 1992, *Mol. Cryst. liq. Cryst.*, **215,** 1.
[5] Göring, P., Diele, S., Fischer, S., Weigeleben, A., Pelzl, G., Stegemeyer, H., and Thyen, W., 1998, *Liq. Cryst.*, **25,** 467.
[6] N'Guyen, H. T., Destrade, C., Levelut, A. M., and Malthète, J., 1986, *J. de Phys.*, **47,** 543.
[7] Alstermark, C., Eriksson, N., Nilsson, M., Destrade, C., and N'Guyen, H. T., 1990, *Liq. Cryst.*, **8,** 75.
[8] Diele, S., Brand, P., and Sackmann, H., 1972, *Mol. Cryst. liq. Cryst.*, **17,** 163.
[9] Levelut, A. M., and Clerc, M., 1998, *Liq. Cryst.*, **24,** 105.
[10] Ukleja, P., Siatkowski, R. E., and Neubert, M. E., 1988, *Phys. Rev. A*, **38,** 4815.
[11] Tardieu, A., and Billard, J., 1976, *J. Phys. Coll.*, **37,** C3-79.
[12] Levelut, A.-M., and Fang, Y., 1991, *Colloq. Phys., No 7*, **23,** C7-229.
[13] Bluce, D. W., Donnio, B., Hudson, S. A., Levelut, A.-M., Megtert, S., Petermann, D., and Veber, M., 1995, *J. Phys. II Fr.*, **5,** 289.
[14] Bluce, D. W., Donnio, B., and Levelut, A.-M., 1997, *Liq. Cryst.*, **22,** 753.
[15] Etherrington, G., Langley, A., Leadbetter, A. J., and Wang, X. J., 1988, *Liq. Cryst.*, **3,** 155.
[16] Tansho, M., Onoda, Y., Kato, R., Kutsumizu, S., and Yano, S., 1998, *Liq. Cryst.*, **24,** 525.
[17] Diele, S., Oelsner, S., Kuschel, F., Hisgen, B., Ringsdorf, H., and Zentel, R., 1987, *Makromol. Chem.*, **188,** 1993.
[18] Nishikawa, E., unpublished results.
[19] Rowell, J. C., Phillips, W. D., Melby, L. R., and Panar, M., 1965, *J. chem. Phys.*, **43,** 3442.
[20] Samulski, E. T., and Luz, Z., 1980, *J. chem. Phys.*, **73,** 142.
[21] Zhou, S., Burger, C., Yeh, F., and Chu, B., 1998, *Macromolecules*, **31,** 8157.
[22] Anderson, D. M., Davis, T. T., and Scriven, L. E., 1990, *Adv. chem. Phys.*, **77,** 337.